Inelastic electron scattering in aggregates of transition metal atoms on metal surfaces

E. C. Goldberg[1,2] and F. Flores[3]

[1]*Instituto de Física del Litoral (CONICET-UNL), Güemes 3450, S3000GLN Santa Fe, Argentina*

[2]*Departamento Ing. Materiales, Facultad de Ing. Química, Universidad Nacional del Litoral, Santiago del Estero 2829, S3000AOM Santa Fe, Argentina*

[3]*Departamento de Física Teórica de la Materia Condensada and IFIMAC, Cantoblanco, Universidad Autónoma, E-28049 Madrid, Spain*

(Received 12 April 2017; revised manuscript received 8 September 2017; published 21 September 2017)

Inelastic spin excitations, as observed with a scanning tunneling microscope for Co/Co and Fe/Fe dimers on a Cu2N/Cu(100) surface, have been analyzed theoretically in this paper. In our approach, we use an extended ionic Hamiltonian for the magnetic atom that takes into account first, the role played by the first Hund rule in the atomic states, and second, the cotunneling processes associated with the atomic excitations and the tunneling conductance. This Hamiltonian is solved using the equation of motion method that yields the appropriate Green's functions allowing us to calculate the differential conductance, the inelastic atomic excitations, and possible Kondo resonances. We also analyze an ideal dimer with spin ½ in each atom and discuss the differences and similarities this model has with the Co-Co case.

DOI: 10.1103/PhysRevB.96.115439

I. INTRODUCTION

Inelastic spin spectroscopy with low-temperature scanning tunneling microscopy [1–5] has been used to explore for magnetic atoms on metals, the intrinsic properties of the corresponding atomic spin in its interaction with the metal free electrons [6]. That interaction might create an antiferromagnetic coupling between the magnetic atom and the metal [7] giving rise to a Kondo resonance, the favorite many-body effect of condensed matter physicists [6].

The conductance spectra obtained by positioning the tip over the magnetic adatom and recording the differential conductance, dI/dV, as a function of the bias potential, V, show different regimes depending on the transition metal located below the tip. Two paradigmatic examples are Fe or Co adsorbed on a Cu2N surface [1–4]: in the case of Co on Cu2N [3], the crystalline field experienced by the atom develops a doublet ground state which is revealed by a Kondo resonance having a temperature of a few degrees. For Fe on Cu2N [2], the magnetic atom develops a singlet ground state, so that the inelastic tunneling differential conductance only shows some steps associated with the internal excitations of the atomic spin and no Kondo resonance.

The success in controlling and understanding the behavior of those individual atoms has stimulated the interest in systems of several units [8,9],which seems to offer interesting developments regarding the understanding of the properties of magnetic systems [10], as well as the building of quantum bits useful for quantum computation [11].

Systems of two units, quantum dots or atoms, interacting with a metal have also attracted broad attention [8] due to the interplay between the possible Kondo resonance of each unit and the ferromagnetic or antiferromagnetic coupling of the spins of the two components. In particular, the cases of two magnetic atoms, such as Co-Fe, Co-Co, or Fe-Fe [12–15], have been analyzed with a scanning tunneling tip showing an important interatomic coupling effect that depends crucially on the distance between atoms; in particular, the tunneling spectroscopy of Fe and Co aggregates reveals the influence of the crystal environment over the atomic magnetocrystalline anisotropy [16]. The interest in analyzing these dimers also stems from the different properties of each individual atom since only Co seems to develop a Kondo resonance.

Several authors have theoretically analyzed this inelastic tunneling problem using different techniques [16–30]. In most of those works an effective interaction between the tunneling electron and the spin of the magnetic atom is introduced; this interaction is described by means of an exchange coupling [16,28], a spin-assisted Hamiltonian [17–19,22–27], or using strong-coupling theory [20,21]. All these approaches are reminiscent of the one used by Kondo [31] to explain the resistivity of dilute magnetic impurities in metals. We can refer to all these cases as approaches that use a kind of effective Kondo Hamiltonian. A different approach to this problem, which has some similarities with our own work, is the one taken by Delgado and Fernández-Rossier [27]; in this paper, the authors start from the Hamiltonian of the isolated magnetic atom for its relevant charge states which include the configurations with a charge q_0, and the ones associated with the charges $q_0 \pm 1$, since the atom is fluctuating between q_0 and $q_0 \pm 1$ in its interaction with the metal; then, after introducing a metal-atom tunneling Hamiltonian, they use degenerate perturbation theory to reduce the initial charge states of the system to an effective Hamiltonian that includes the hopping between the electrodes assisted by the excitation of the atom between the states of the q_0 manifold. This perturbation theory yields a kind of generalized Kondo Hamiltonian where, instead of the spin states, $|S,M\rangle$, one finds the q_0-configurational states. Using the authors' own words: "this approach provides a microscopic justification of earlier phenomenological works".

It is also appropriate to mention that in Refs. [29,30] a similar proposal as in Ref. [27] is solved for a single atom by using a nonperturbative treatment of the generalized Anderson Hamiltonian within the so-called one-crossing approximation [32].

Our approach to analyze this problem also starts from the atomic Hamiltonian for the q_0 and $q_0 \pm 1$ charges; but, instead of integrating out the $q_0 \pm 1$ states, we introduce an ionic Hamiltonian [33] that reduces the q_0 and $q_0 \pm 1$ configurational states to those associated with the first Hund

rule. In a second step, we use the spin symmetry of those states to obtain the atom-metal interaction as a function of only one parameter that defines the coupling between the metal and the atom. Finally, we analyze our Anderson-like Hamiltonian using an equation of motion (EOM) method combined with Green's function techniques which keep, in principle, all the possible cotunneling processes associated with the q_0 and $q_0 \pm 1$ charge states. We stress that, up to now, all the different theoretical approaches to this inelastic electron tunneling problem for a dimer use a kind of Kondo Hamiltonian; our approach is the only one that keeps track of all the atomic fluctuating processes in a very detailed Anderson-like Hamiltonian. In other words, in our Anderson-like approach, the tunneling conductance is the result of a cotunneling process [27], whereby electrons jump successively first from one electrode to the atom and, in a second step, from the atom to the other electrode; in the Kondo-like Hamiltonians, electrons jump between electrodes simultaneously exciting the magnetic atom along this jump.

We should mention that using this formalism we have already successfully analyzed individual Co or Fe magnetic atoms [34] as well as the Fe/Co dimer [35]. In these works, we introduced for each atom the above-mentioned ionic Hamiltonian complemented with other terms that take into account the Zeeman and the magnetocrystalline anisotropy effects, as well as the Heisenberg coupling between spins. In this work we theoretically analyze the Fe/Fe and the Co/Co dimers using a similar approach, and discuss the differential conductance across the system as measured by the tip of a scanning tunnel microscope. The major interest in analyzing these cases comes from the Co-Co dimer, because due to the degenerate states responsible for the Kondo resonance appearing for the individual Co atoms, the approximations used in [35] for calculating the appropriate Green's functions are not good enough, and we have been forced to go to a higher approximation, as discussed below in detail.

We also present results for a dimer formed by equal atoms which are assumed to each have a 1/2 spin; this case might be considered a simplified model of the Co-Co case, since each atom presents a doublet ground state. Apparently, the doublet might be simulated by a ½ spin, and the Co-Co dimer by a 1/2-1/2 system; we will discuss, however, the similarities and differences between these two cases.

The paper is organized as follows: in Secs. II and III we present our basic Hamiltonian for one magnetic atom and an aggregate of atoms interacting with a metal surface. In Sec. IV the equation of motion method for solving those Hamiltonians is discussed. In Sec. V, we show how to obtain the tunneling current across the magnetic atom from the previous solution. Then, the formalism is applied to the 1/2-1/2 case in Sec. VI. In Sec. VII we discuss the similarities and differences between the 1/2-1/2 case and a simplified Co/Co dimer. In Sec. VIII we present our results for the Co-Co and Fe-Fe dimers; and finally, in Sec. IX we present our conclusions.

II. ONE ATOM INTERACTING WITH METAL SURFACES

We start presenting our Hamiltonian for describing the atomic orbitals, the metal states, and the interaction between the atom and those states:

$$\hat{H} = \sum_{k\alpha\sigma} \varepsilon_{k\alpha} \hat{n}_{k\alpha\sigma} + \hat{H}_{\text{atom}} + \hat{H}_{\text{int}}. \tag{1}$$

In Eq. (1), the first term describes the substrate ($\alpha = s$) and tip ($\alpha = t$). These metal surfaces are described by the conduction-band energies $\varepsilon_{k\alpha}$ and their occupation number given by $\hat{n}_{k\alpha\sigma} = \hat{c}^{+}_{k\alpha\sigma}\hat{c}_{k\alpha\sigma}$ [index k may include more than one band: $k \equiv (k_1, k_2, \ldots)$]. The atomic part, $\hat{H}_{\text{atom}}$, in the extended version appropriate for treating any multielectron atom [36], is given by

$$\begin{aligned}\hat{H}_{\text{atom}} = &\sum_{m,\sigma} \varepsilon_m \hat{n}_{m\sigma} + \sum_{m} U_d \hat{n}_{m\uparrow}\hat{n}_{m\downarrow} \\ &+ \frac{1}{2}\sum_{m\neq m',\sigma} J_d \hat{n}_{m\sigma}\hat{n}_{m'-\sigma} \\ &+ \frac{1}{2}\sum_{m\neq m',\sigma} \left(J_d - J^x_d\right)\hat{n}_{m\sigma}\hat{n}_{m'\sigma} \\ &- \frac{1}{2}\sum_{m\neq m',\sigma} J^x_d \hat{c}^{\dagger}_{m\sigma}\hat{c}_{m-\sigma}\hat{c}^{\dagger}_{m'-\sigma}\hat{c}_{m'\sigma}. \end{aligned} \tag{2}$$

Here $\hat{c}^{\dagger}_{m\sigma}$ ($\hat{c}_{m\sigma}$) are the fermionic operators creating (annihilating) an electron with spin projection σ in the orbital m and $\hat{n}_{m\sigma} = \hat{c}^{\dagger}_{m\sigma}\hat{c}_{m-\sigma}$; the intra-atomic Coulomb interactions U_d and J_d, as well as the intra-atomic exchange interaction J^x_d, are assumed to be constants independent of the m-orbital index, and $\varepsilon_m = \varepsilon_0$ also independent of m. The last term, related to spin-flip processes, restores the invariance under rotation in spin space. Other contributions, such as crystal field effects and the Zeeman energy terms associated with an applied magnetic field are not included in Eq. (2), but will be discussed below.

The interaction term, $\hat{H}_{\text{int}}$, contemplates the charge exchange between the atom and the metal surfaces through a one-electron tunneling mechanism described by the following expression:

$$\hat{H}_{\text{int}} = \sum_{k\alpha,m,\sigma} [V_{k\alpha m}\hat{c}^{\dagger}_{k\alpha\sigma}\hat{c}_{m\sigma} + V_{mk\alpha}\hat{c}^{\dagger}_{m\sigma}\hat{c}_{k\alpha\sigma}]. \tag{3}$$

In the case of the d orbitals of metal transition atoms, it is a good approximation to assume the exchange interaction, J^x_d, large enough to make the first Hund-rule operative. On the other hand, we also assume that the orbital contribution to the angular moment is quenched due to crystal-field effects and the low symmetry of the atom environment. These conditions imply that the ground state of the atom is an orbital singlet, and that its lower energy configurations correspond to the states of maximum electron spin, S, associated with its number of electrons, N, that in the Introduction was mentioned as the equivalent q_0 states [27].

Based on these arguments, the atomic Hamiltonian [Eq. (2)] is projected over the Hund's states of total spin S and spin projection M, $|S,M\rangle$. Notice that by introducing Hund's states $|S,M\rangle$ we reduce the full configuration space spanned by Hamiltonian (2) to the one spanned by those states, so that in our calculations it is assumed that $\sum_{S,M} |S,M\rangle\langle S,M| = 1$.This is the main simplification introduced in our

approach:

$$\hat{H}_{\text{atom}} = \sum_{S,M} E^S |S,M\rangle\langle S,M|. \tag{4a}$$

The total energies E^S calculated from the atomic Hamiltonian, Eq. (2), are given by

$$\begin{aligned} E^S = & \sum_{m,\sigma} \varepsilon_m \langle \hat{n}_{m\sigma}\rangle_{S,M} + \sum_m U_d \langle \hat{n}_{m\uparrow}\hat{n}_{m\downarrow}\rangle_{S,M} \\ & + \frac{1}{2}\sum_{m\neq m',\sigma} J_d \langle \hat{n}_{m\sigma}\hat{n}_{m'-\sigma}\rangle_{S,M} \\ & + \frac{1}{2}\sum_{m\neq m',\sigma} \left(J_d - J_d^x\right)\langle \hat{n}_{m\sigma}\hat{n}_{m'\sigma}\rangle_{S,M} \\ & - \frac{1}{2}\sum_{m\neq m',\sigma} J_d^x \langle \hat{c}^\dagger_{m\sigma}\hat{c}_{m-\sigma}\hat{c}^\dagger_{m'-\sigma}\hat{c}_{m'\sigma}\rangle_{S,M}, \end{aligned} \tag{4b}$$

$\langle\cdots\rangle_{S,M}$ being the average value in the $|S,M\rangle$ state.

Regarding the interaction term, Eq. (3), we assume that in the most general case, the ground state with N electrons, $|S,M\rangle$, may fluctuate not only to a state with $N-1$ electrons, $|S-1/2,M\rangle$, but also to a state with $N+1$, $|S+1/2,M\rangle$ ($N<5$):

$$\begin{aligned} \hat{H}_{\text{int}} = & \sum_{k\alpha,M,\sigma} \left[V^{S*}_{k\alpha M\sigma}\hat{c}^\dagger_{k\alpha\sigma}|S-1/2,M-\sigma\rangle\langle S,M| \right. \\ & \left. + V^S_{k\alpha M\sigma}|S,M\rangle\langle S-1/2,M-\sigma|\hat{c}_{k\alpha\sigma}\right] \\ & + \sum_{k\alpha,M,\sigma}\left[V'^{S+1/2*}_{k\alpha M\sigma}\hat{c}^\dagger_{k\alpha\sigma}|S,M-\sigma\rangle\langle S+1/2,M| \right. \\ & \left. + V'^{S+1/2}_{k\alpha M\sigma}|S+1/2,M\rangle\langle S,M-\sigma|\hat{c}_{k\alpha\sigma}\right]. \end{aligned} \tag{5}$$

A similar equation holds for $N>5$. The different spin states $|S,M\rangle$ are calculated by rotating the spin, which means that they are generated from the state $|S,S\rangle$ by successive applications of the operator $\hat{S}^-$. In this way the following expression for the coupling terms, $V^S_{kM\sigma}$ in Eq. (5), is obtained for the case of a half-filled or less than half-filled shell ($N\leqslant 5$ for a d shell) [34]:

$$V^S_{kM\sigma} = \sqrt{\frac{S+(-1)^p M}{2S}}V_{kd}, \tag{6}$$

while for an occupation larger than a half-filled shell ($N>5$ for a d shell), we arrive at the expression

$$V^S_{kM\sigma} = (-1)^p\sqrt{\frac{S-(-1)^p M}{2S}}V_{kd}. \tag{7}$$

In Eqs. (6) and (7), p is equal to 0 if $\sigma = 1/2$ and equal to 1 if $\sigma = -1/2$.

We should stress that Eq. (5) for $N<5$ defines an Anderson-like Hamiltonian, where different terms have one $\hat{c}^\dagger_{k\sigma}$-creation (or $\hat{c}_{k\sigma}$-annihilation) operator and a $|S-1/2,M-\sigma\rangle\langle S,M|$-annihilation (or a $|S\rangle\langle S-1/2|$-creation) operator. The operators $|S-1/2\rangle\langle S|$ destroy one electron, for $N<5$, in state $|S\rangle$, making the atom jump to state $|S-1/2\rangle$; likewise the operators $|S+1/2\rangle\langle S|$ create one electron, for $N<5$, in state $|S\rangle$ making the atom jump to the state $|S+1/2\rangle$. Notice that those operators are fermionlike because $|S\rangle$ and $|S\pm 1/2\rangle$ differ by one electron. However, operators such as $|S,M\rangle\langle S,M'|$ or $|S\pm 1/2,M\rangle\langle S\pm 1/2,M'|$ are bosons (see Ref. [37] to see the properties of these operators). Consequently, Eqs. (5)–(7) define an Anderson-like interacting Hamiltonian that depends only on one parameter, V_{kd}, very much like the simplest Anderson Hamiltonian introduced for a 1/2-spin particle. This is the main advantage of our ionic Hamiltonian [38], namely, that it does not depend on so many parameters as the initial ionic model.

The interaction Hamiltonian, Eq. (5), depicts the cotunneling processes in which one electron or one hole can tunnel from one lead to the atom and at the same time, another electron or hole can tunnel from the atom to the other lead. An inelastic scattering process occurs when the initial and final states of total spin S have different energies. The transitions to the virtual intermediate states with either total spin $S+1/2$ or $S-1/2$ do not conserve energy, but the time spent in these intermediate states is coherent with that predicted by the uncertainty principle [39].

In general, the electronic and chemical properties of the atom-surface system, as described by our Hamiltonian, depend on the coupling parameter V_{kd} and the one-electron energies involved in the charge-exchange process: $E^S - E^{S-1/2} = J_d - J_d^x + \varepsilon_0$ for $N\leqslant 5$ and $E^S - E^{S-1/2} = -(J_d - J^x{}_d) - \varepsilon_0$ for $N>5$.

The atom-surface coupling, V_{kd}, in Eqs. (6) and (7) depends on the atomic configurations associated with the metal/atom charge-exchange processes. In order to substantiate further these assumptions, consider the Fe/CuN(100) case; some density functional theory calculations [2,40] indicate that the largest occupation for the minority spins appears for the $d_{x^2-y^2}$ and d_{z^2} orbitals with occupancies of 0.72 and 0.49 electrons, respectively (assuming the z axis in the direction perpendicular to the surface).

On the other hand, the excited configurations with $S=2$ obtained by considering the crystal-field effects are separated more than 300 meV from the ground state and can be disregarded as possible inelastic channels in the conductance spectra around the surface Fermi energy, that only extends up to 50 mV [14]. Therefore, by considering the following orbital ordering $|d_{x^2-y^2},d_{z^2},d_{zy},d_{xy},d_{zx}\rangle$, the Fe ground state is $|S=2,M=2\rangle = |\uparrow\downarrow,0\uparrow,0\uparrow,0\uparrow,0\uparrow\rangle$ and the atom can fluctuate to the state $|S=3/2,M=3/2\rangle = |\uparrow\downarrow,\uparrow\downarrow,0\uparrow,0\uparrow,0\uparrow\rangle$ by exchanging one electron with the metal (spin rotation states are understood to be included in the space spanned by $|S=2,M\rangle$ and $|S=3/2,M'\rangle$). Then, in this case V_{kd} represents the coupling between the d_{z^2} orbital and the metal k state. An explicit calculation of the interacting hopping elements between the different $|S=3/2,M\rangle$ and $|S=2,M'\rangle$ states yields the values of Eq. (7) ($N>5$).

We should say that independent calculations by Etzkorn *et al.* [41] indicate that there are some small contributions from the spin-orbit interaction to the angular moment of Fe and Co deposited on the Cu site (the most likely adsorption site). That orbital momentum is calculated to be around 0.2 μ_B for Fe and 0.4 μ_B for Co; these values suggest that assuming that the ground state of those atoms is an orbital singlet is a

fair approximation, as confirmed independently by the good agreement we find with the experimental results.

All eigenstates E^S of Hamiltonian (4) are degenerate in M. This degeneracy is, however, partially lifted when the following terms are added to the atomic Hamiltonian:

$$\hat{H}_p = g\mu_B \hat{B}\cdot\hat{S} + DS_z^2 + E\left(S_x^2 - S_y^2\right). \tag{8}$$

The first term in Eq. (8) is associated with the Zeeman energy (g is the gyromagnetic factor and μ_B the Bohr magneton); the other two with the effective anisotropy interaction $\Lambda_{ij}\hat{S}_i\cdot\hat{S}_j$ which comes from a second-order perturbative calculation of the atomic spin-orbit coupling $\lambda\hat{L}.\hat{S}$**.** We should stress that this perturbation treatment includes contributions coming from virtual transitions between states with $L = 0$ and $L \neq 0$ which are not included in our simplified Hamiltonian [14,15]; this means that the effective anisotropy interaction can be viewed as an extra term to be added to our Hamiltonian (4a).

Leaving apart Hamiltonian (8), $\hat{H}_p$, our ionic Hamiltonian as defined by Eqs. (4) and (5) leads to an effective metal/atom exchange coupling that keeps the rotational symmetry of the problem, giving an independent confirmation to the validity of this approach. This can be proved by applying the Schrieffer-Wolf transformation [42], assuming $\hat{H}_{\rm int}$ small and using a second-order perturbation theory [7].

III. AGGREGATES OF ATOMS INTERACTING WITH A METAL SURFACE

In this section we consider the case of many atoms ($\alpha = 1,2,\ldots,n$), distributed parallel to the surface, then, if for each atom α, we have the electronic configuration $|S_\alpha M_\alpha\rangle$, we also have the completeness condition $\Sigma_\alpha |S_\alpha M_\alpha\rangle\langle S_\alpha M_\alpha| = 1$. The extension of Eqs. (4) and (5) to the case of many noninteracting atoms is straightforward by considering the direct product of the different states for each atom:

$$|S_a M_a; S_b M_b; S_c M_c; \ldots\rangle = |S_a M_a\rangle \otimes |S_b M_b\rangle \otimes |S_c M_c\rangle \otimes \ldots.$$

The one-electron tunneling mechanism of charge transfer [Eq. (3)] means in this case that the charge fluctuation in atom b is occurring without change in the electronic configurations of the other atoms. Then, the interaction Hamiltonian, Eq. (5), in the particular case of two atoms, is straightforwardly extended to the form

$$\begin{aligned}
\hat{H}_{\rm int} = &\sum_{k\beta,M_1,M_2,\sigma} \left[V^{S_1 *}_{k\beta M_1\sigma}\hat{c}^\dagger_{k\beta\sigma}|S_1 - 1/2 M_1 - \sigma; S_2 M_2\rangle\langle S_1 M_1; S_2 M_2| + \text{c.c.}\right] \\
&+ \sum_{k\beta,M_1,M_2,\sigma} \left[V'^{2S_1+1/2 *}_{k\beta M_1\sigma}\hat{c}^\dagger_{k\beta\sigma}|S_1 M_1 - \sigma; S_2 M_2\rangle\langle S_1 + 1/2 M_1; S_2 M_2| + \text{c.c.}\right] \\
&+ \sum_{k\beta,M_1,M_2,\sigma} (-1)^{2S_1}\left[V^{S_2 *}_{k\beta M_2\sigma}\hat{c}^\dagger_{k\beta\sigma}|S_1 M_1; S_2 - 1/2 M_2 - \sigma\rangle\langle S_1 M_1; S_2 M_2| + \text{c.c.}\right] \\
&+ \sum_{k\beta,M_1,M_2,\sigma} (-1)^{2S_1}\left[V'^{2S_2+1/2 *}_{k\beta M_2\sigma}\hat{c}^\dagger_{k\beta\sigma}|S_1 M_1; S_2 M_2 - \sigma\rangle\langle S_1 M_1; S_2 + 1/2 M_2| + \text{c.c.}\right].
\end{aligned} \tag{9}$$

Equation (9) is written in the basis set which diagonalizes the system of noninteracting atoms. In the next step we write the interaction Hamiltonian in the basis set $\{\psi_j^{S_1,S_2}\}$ that diagonalizes the following atomic Hamiltonian:

$$\hat{H}_{\rm atom} = \sum_{S_i,M_i} E^{S_i}|S_i,M_i\rangle\langle S_i,M_i| + \sum_i \left[D_i S_{iz}^2 + E_i\left(S_{ix}^2 - S_{iy}^2\right)\right] + \sum_i g_i\mu_B\hat{B}\cdot\hat{S}_i + \sum_{i\neq j} J_{ij}\hat{S}_i\cdot\hat{S}_j, \tag{10}$$

which includes the anisotropy term, the interaction with an external magnetic field $\hat{B}$(third term), and a Heisenberg exchange interaction between atoms (fourth term). It should be commented that this last interaction is in principle contemplated by our Hamiltonian. However, this interaction can be shown to be of fourth order in the interaction V_{kd} [43], while the calculations we are going to present in the next sections are performed to second order in V_{kd}; therefore, there is no inconsistency in our approach. If our calculations were extended to all the fourth-order terms in V_{kd}, one should take away the interaction $\sum_{i,j} J_{ij}\hat{S}_i\cdot\hat{S}_j$.

Let us consider from now on the case of two atoms and assume that we have in each atom only spin fluctuations from S to S-1/2; then, the interaction Hamiltonian (9), projected over the basis set that contemplates the mixing of the noninteracting many-body states, $|\psi_j^{S_1,S_2}\rangle = \sum_{M_1,M_2} a_{M_1,M_2}^{j(S_1,S_2)}|S_1 M_1, S_2 M_2\rangle$, takes the form

$$\begin{aligned}
\hat{H}_{\rm int} = &\sum_{k\alpha,\sigma,i,j} \left[T^{S_1\to S_1-1/2,S_2 *}_{k\alpha\sigma ij}\hat{c}^\dagger_{k\alpha\sigma}\left|\psi_i^{S_1-1/2,S_2}\right\rangle\left\langle\psi_j^{S_1,S_2}\right| + \text{c.c.}\right] \\
&+ \sum_{k\alpha,\sigma,i,j} \left[T^{S_1\to S_1-1/2,S_2-1/2 *}_{k\alpha\sigma ij}\hat{c}^\dagger_{k\alpha\sigma}\left|\psi_i^{S_1-1/2,S_2-1/2}\right\rangle\left\langle\psi_j^{S_1,S_2-1/2}\right| + \text{c.c.}\right] \\
&+ \sum_{k\alpha,\sigma,i,j} (-1)^{2S_1}\left[T^{S_1,S_2\to S_2-1/2 *}_{k\alpha\sigma ij}\hat{c}^\dagger_{k\alpha\sigma}\left|\psi_i^{S_1,S_2-1/2}\right\rangle\left\langle\psi_j^{S_1,S_2}\right| + \text{c.c.}\right] \\
&+ \sum_{k\alpha,\sigma,i,j} (-1)^{2(S_1-1/2)}\left[T^{S_1-1/2,S_2\to S_2-1/2 *}_{k\alpha\sigma ij}\hat{c}^\dagger_{k\alpha\sigma}\left|\psi_i^{S_1-1/2,S_2-1/2}\right\rangle\left\langle\psi_j^{S_1-1/2,S_2}\right| + \text{c.c.}\right].
\end{aligned} \tag{11}$$

This is an Anderson-like Hamiltonian, where $\hat{c}^{\dagger}_{k\alpha\sigma}|\psi_i^{S_1-1/2,S_2}\rangle\langle\psi_j^{S_1,S_2}|$, for example, is the product of a creation operator, $\hat{c}^{\dagger}_{k\alpha\sigma}$, and an annihilation one $|\psi_i^{S_1-1/2,S_2}\rangle\langle\psi_j^{S_1,S_2}|$; with this term, the many-body atom system changes from the state $|\psi_j^{S_1,S_2}\rangle$ to the state $|\psi_i^{S_1-1/2,S_2}\rangle$, due to the electron transfer from the atom 1 with total spin S_1 to the surface. The coupling parameters are redefined as

$$T^{S_1\to S_1-1/2,S_2}_{k\alpha\sigma ij} = \sum_{m_1m_2M_2} a^{j(S_1,S_2)*}_{m_1m_2} a^{i(S_1-1/2,S_2)}_{m_1-\sigma M_2} V^{S_1}_{k\alpha m_1\sigma}. \quad (12)$$

This Anderson-like Hamiltonian allows us to calculate the tunneling current through the Co-Co or the Fe-Fe dimers, as well as the electronic properties associated with their Kondo resonances; this is at variance with many other approaches where a phenomenological Kondo-like Hamiltonian depending on different parameters has been used [22–24]. The accuracy of the results obtained from Eq. (11) depends on the quality of the approach used to solve it.

We analyze Hamiltonian (11) by means of a Green's function approach, combined with an EOM technique, associated with the different annihilation and creation operators: $|\psi_i{}^{S-1/2,S'}\rangle\langle\psi_j{}^{S,S'}|$,$|\psi_i{}^{S,S'-1/2}\rangle\langle\psi_j{}^{S,S'}|$, $\ldots,|\psi_i{}^{S,S'}\rangle\langle\psi_j{}^{S,S'-1/2}|\ldots$, appearing in that Hamiltonian. It is convenient to realize that the spin fluctuation $S \leftrightarrow S-1/2$ in atom A can occur in the presence of the other atom B with either spin s or spin s-1/2; and the same is valid for the spin fluctuation in atom B (S is used now for atom A and s for atom B, instead of S_1 and S_2). These two possibilities can be identified with the following "creation" operators ($N < 5$):

$$\hat{A}^{(1)\dagger}_{ij} = |\psi_i^{S,s}\rangle\langle\psi_j^{S-1/2,s}|;$$
$$\hat{A}^{(2)\dagger}_{ij} = |\psi_i^{S,s-1/2}\rangle\langle\psi_j^{S-1/2,s-1/2}|$$
$$\hat{B}^{(1)\dagger}_{ij} = |\psi_i^{S,s}\rangle\langle\psi_j^{S,s-1/2}|;$$
$$\hat{B}^{(2)\dagger}_{ij} = |\psi_i^{S-1/2,s}\rangle\langle\psi_j^{S-1/2,s-1/2}|. \quad (13)$$

Then, the appropriate Green's functions for calculating the electronic transport properties for each atom, close to the equilibrium, must contemplate the two-atom system with the two possible spin fluctuations in each atom. That means one has to solve a matrix of 16 elements (see below) defined by the blocks $[A^{(\alpha)}A^{(\beta)}]$, $[A^{(\alpha)}B^{(\beta)}]$, $[B^{(\alpha)}B^{(\beta)}]$, and $[B^{(\alpha)}A^{(\beta)}]$. In other words, we need to calculate Green's functions such as those defined in the first two blocks (for the second two blocks the Green's functions are completely similar):

$$G_{A^{\alpha}_{ij}}\left(\hat{A}^{(\beta)}_{qp}\right) = i\Theta(t'-t)\left\langle\left\{\hat{A}^{(\alpha)\dagger}_{ij}(t');\hat{A}^{(\beta)}_{qp}(t)\right\}\right\rangle, \quad (14a)$$
$$G_{A^{\alpha}_{ij}}\left(\hat{B}^{(\beta)}_{qp}\right) = i\Theta(t'-t)\left\langle\left\{\hat{A}^{(\alpha)\dagger}_{ij}(t');\hat{B}^{(\beta)}_{qp}(t)\right\}\right\rangle, \quad (14b)$$

where $\{\ldots\}$ is the anticonmutator of the two operators inside the brackets.

The first ones [Eq. (14a)] are diagonal in site, and for $\alpha=\beta$, are also diagonal in the spin configuration that fluctuates; while the second, Eq. (14b), corresponds to off-diagonal atomic Green's functions.

The normalization of the space of configurations requires fulfilling the following relation:

$$\sum_i \left\langle\left|\psi_i^{S,s}\right\rangle\left\langle\psi_i^{S,s}\right|\right\rangle + \sum_j \left\langle\left|\psi_j^{S-1/2,s}\right\rangle\left\langle\psi_j^{S-1/2,s}\right|\right\rangle + \sum_j \left\langle\left|\psi_j^{S,s-1/2}\right\rangle\left\langle\psi_j^{S,s-1/2}\right|\right\rangle + \sum_j \left\langle\left|\psi_j^{S-1/2,s-1/2}\right\rangle\right.$$
$$\left.\times\left\langle\psi_j^{S-1/2,s-1/2}\right|\right\rangle = 1.$$

IV. EOM METHOD FOR CALCULATING THE GREEN'SFUNCTIONS

Here, we describe the procedure for calculating one particular Green's function. We assume that the interaction of the atom with the tip is negligible compared with the interaction with the substrate (tunneling regime). In this case the atom spectral density is determined by the atom-substrate interaction, while the current through the atom is determined by the coupling between the tip and the atom. Then, from now on we will only refer to the atom interaction with the substrate band states in the calculation of the Green's functions and by simplicity, we omit the subindex $\alpha = s$.

Taking into account the time-dependent evolution of the Heisenberg operators, $d\hat{A}^{(1)}_{qp}/dt = -i[\hat{A}^{(1)}_{qp},\hat{H}]$, and the orthonormality of the many-body functions $\psi_i^{S_1,S_2}$, we can write (Z^{α}_{ij} corresponds to either A or B)

$$idG_{Z^{\alpha}_{ij}}\left(\hat{A}^{(1)}_{qm}\right)/dt = \delta(t-t')\left\langle\left\{\hat{Z}^{(\alpha)}_{ij},\hat{A}^{(1)}_{qm}\right\}\right\rangle + i\Theta(t'-t)\left\langle\left\{\hat{Z}^{(\alpha)}_{ij},\left[\hat{A}^{(1)}_{qm},\hat{H}\right]\right\}\right\rangle,$$

where $[\ldots]$ is the commutator of the operators inside the brackets, in such a way that the time derivative of the Green's function $G_{Z^{\alpha}_{ij}}(\hat{A}^{(1)}_{qm})$ is

$$idG_{Z^{\alpha}_{ij}}\left(\hat{A}^{(1)}_{qm}\right)/dt = \delta(t-t')\left\langle\left\{\hat{Z}^{(\alpha)}_{ij}(t'),\hat{A}^{(1)}_{qm}(t)\right\}\right\rangle + \left(E^{S,s}_q - E^{S-1/2,s}_m\right)G_{Z^{\alpha}_{ij}}\left(\hat{A}^{(1)}_{qm}\right) + \sum_{k,\sigma,n} T^{A^1}_{k\sigma nq} G_{Z^{\alpha}_{ij}}\left(\left|\psi_m^{S-1/2,s}\right\rangle\left\langle\psi_n^{S-1/2,s}\right|\hat{c}_{k\sigma}\right)$$
$$+ \sum_{k,\sigma,n} T^{A^1}_{k\sigma mn} G_{Z^{\alpha}_{ij}}\left(\left|\psi_n^{S,s}\right\rangle\left\langle\psi_q^{S,s}\right|\hat{c}_{k\sigma}\right) + (-1)^{2S}\sum_{k,\sigma,n} T^{B^1}_{k\sigma nq} G_{Z^{\alpha}_{ij}}\left(\left|\psi_m^{S-1/2,s}\right\rangle\left\langle\psi_n^{S,s-1/2}\right|\hat{c}_{k\sigma}\right) - (-1)^{2S-1}$$
$$\times \sum_{k,\sigma,n} T^{B^2}_{k\sigma nm} G_{Z^{\alpha}_{ij}}\left(\hat{c}^{\dagger}_{k\sigma}\left|\psi_n^{S-1/2,s-1/2}\right\rangle\left\langle\psi_q^{S,s}\right|\right). \quad (15)$$

Notice that the different Green's function components of this equation come from different transitions like such as $\hat{A}^{(1)}_{mq} = |\psi_m^{S-1/2,s}\rangle\langle\psi_q^{S,s}| \rightarrow \hat{c}^\dagger_{k\sigma}|\psi_n^{S-1/2,s-1/2}\rangle\langle\psi_q^{S,s}|$, where an electron k is transferred to the metal from the state $|\psi_m^{S-1/2,s}\rangle$ which jumps to the state $|\psi_n^{S-1/2,s-1/2}\rangle$.

In the next step, we calculate the time derivative of each new Green's function which appears in Eq. (15). After introducing mean-field approximations like this one:

$$G_{Z^\alpha_{ij}}\big(\hat{B}^{(2)}_{pn}\hat{n}_{k\sigma}\big) \approx \langle\hat{n}_{k\sigma}\rangle G_{Z^\alpha_{ij}}\big(\hat{B}^{(2)}_{pn}\big),$$

for example, the equation for the Green's function $G_{Z^\alpha_{ij}}(\hat{c}^\dagger_{k\sigma}|\psi_n^{S-1/2,s-1/2}\rangle\langle\psi_q^{S,s}|)$ yields

$$\begin{aligned} i dG_{Z^\alpha_{ij}}\big(\hat{c}^\dagger_{k\sigma}\big|\psi_n^{S-1/2,s-1/2}\big\rangle\big\langle\psi_q^{S,s}\big|\big)/dt &= \delta(t-t')\big\langle\big\{\hat{Z}^{(\alpha)}_{ij},\hat{c}^\dagger_{k\sigma}\big|\psi_n^{S-1/2,s-1/2}\big\rangle\big\langle\psi_q^{S,s}\big|\big\}\big\rangle \\ &+ \big(E_q^{S,s} - E_n^{S-1/2,s-1/2} - \varepsilon_k\big)G_{Z^\alpha_{ij}}\big(\hat{c}^\dagger_{k\sigma}\big|\psi_n^{S-1/2,s-1/2}\big\rangle\big\langle\psi_q^{S,s}\big|\big) \\ &- \sum_p T^{A^1}_{k\sigma pq}\langle\hat{n}_{k\sigma}\rangle G_{Z^\alpha_{ij}}\big(\hat{B}^{(2)}_{pn}\big) - (-1)^{2S}\sum_p T^{B^1}_{k\sigma pq}\langle\hat{n}_{k\sigma}\rangle G_{Z^\alpha_{ij}}\big(\hat{A}^{(2)}_{pn}\big) \\ &- \sum_p T^{A^2}_{k\sigma np}\langle 1-\hat{n}_{k\sigma}\rangle G_{Z^\alpha_{ij}}\big(\hat{B}^{(1)}_{qp}\big) - (-1)^{2S-1}\sum_p T^{B^2}_{k\sigma np}\langle 1-\hat{n}_{k\sigma}\rangle G_{Z^\alpha_{ij}}\big(\hat{A}^{(1)}_{qp}\big), \end{aligned} \tag{16}$$

where, again, new Green's functions appear due to transitions from $\hat{c}^\dagger_{k\sigma}|\psi_n^{S-1/2,s-1/2}\rangle\langle\psi_q^{S,s}|$ to annihilation operators such as $B^{(2)}_{pn} = |\psi_n^{S-1/2,s-1/2}\rangle\langle\psi_p^{S-1/2,s}|$ and $\hat{A}^{(1)}_{pq} = |\psi_n^{S-1/2,s}\rangle\langle\psi_q^{S,s}|$. By Fourier transforming Eq. (16) and inserting it in the Fourier transform of Eq. (15), we finally obtain the following equation ($Z^\alpha_{ij} = A^1_{ij}$):

$$\begin{aligned} g_0^{-1}\big(\hat{A}^{(1)}_{qm}\big)G_{A^1_{ij}}\big(\hat{A}^{(1)}_{qm}\big) &= \big\langle\big|\psi_q^{S,s}\big\rangle\big\langle\psi_i^{S,s}\big|\delta_{jm} + \big|\psi_j^{S-1/2,s}\big\rangle\big\langle\psi_m^{S-1/2,s}\big|\delta_{iq}\big\rangle \\ &+ \sum_{k,\sigma,n}\frac{T^{A^1}_{k\sigma nq}\big\langle\hat{A}^{(1)\dagger}_{in}\hat{c}_{k\sigma}\big\rangle}{\omega-\varepsilon_k-E_n^{S-1/2,s}+E_j^{S-1/2,s}}\delta_{jm} + (-1)^{2S}\sum_{k,\sigma,p}\frac{T^{B^1}_{k\sigma pq}\big\langle\hat{B}^{(1)\dagger}_{ip}\hat{c}_{k\sigma}\big\rangle}{\omega-\varepsilon_k-E_p^{S,s-1/2}+E_j^{S-1/2,s}}\delta_{jm} \\ &- \sum_{k,\sigma,p}\frac{T^{A^1}_{k\sigma mp}\big\langle\hat{A}^{(1)\dagger}_{pj}\hat{c}_{k\sigma}\big\rangle}{\omega-\varepsilon_k-E_i^{S,s}+E_p^{S,s}}\delta_{qi} - (-1)^{2S-1}\sum_{k,\sigma,l}\frac{T^{B^2}_{k\sigma lm}\big\langle\hat{c}^\dagger_{k\sigma}\hat{B}^{(2)}_{jl}\big\rangle}{\omega+\varepsilon_k-E_q^{S,s}+E_l^{S-1/2,s-1/2}}\delta_{qi} \\ &+ \sum_{p\neq m}\Xi^{A^1(I)}_{qp}(\omega)G_{A^1_{ij}}\big(\hat{A}^{(1)}_{qp}\big) + \sum_{p\neq q}\Xi^{A^1(II)}_{pm}(\omega)G_{A^1_{ij}}\big(\hat{A}^{(1)}_{pm}\big) - \sum_{p,l}\Xi^{A^2}_{pl}(\omega)G_{A^1_{ij}}\big(\hat{A}^{(2)}_{pl}\big) \\ &+ (-1)^{2S}\sum_p\Xi^{B^1}_{qp}(\omega)G_{A^1_{ij}}\big(\hat{B}^{(1)}_{qp}\big) + (-1)^{2S-1}\sum_{l,p}\Xi^{B^2}_{lp}(\omega)G_{A^1_{ij}}\big(\hat{B}^{(2)}_{lp}\big) \end{aligned} \tag{17}$$

where we have defined

$$\begin{aligned} g_0^{-1}\big(\hat{A}^{(1)}_{qm}\big) &= \omega - E_q^{S,s} + E_m^{S-1/2,s} - \sum_{k,\sigma,n}\frac{\big|T^{A^1}_{k,\sigma,n,q}\big|^2\langle 1-\hat{n}_{k\sigma}\rangle}{\omega-\varepsilon_k-E_n^{S-1/2,s}+E_m^{S-1/2,s}} - \sum_{k,\sigma,n}\frac{\big|T^{A^1}_{k,\sigma,m,n}\big|^2\langle\hat{n}_{k\sigma}\rangle}{\omega-\varepsilon_k-E_q^{S,s}+E_n^{S,s}} \\ &- \sum_{k,\sigma,n}\frac{\big|T^{B^1}_{k,\sigma,n,q}\big|^2\langle 1-\hat{n}_{k\sigma}\rangle}{\omega-\varepsilon_k-E_n^{S,s-1/2}+E_m^{S-1/2,s}} - \sum_{k,\sigma,l}\frac{\big|T^{B^2}_{k,\sigma,l,m}\big|^2\langle 1-\hat{n}_{k\sigma}\rangle}{\omega+\varepsilon_k-E_q^{S,s}+E_l^{S-1/2,s-1/2}}. \end{aligned} \tag{18}$$

The expressions of the crossed atom-band state terms such as $\langle\hat{A}^{(1)\dagger}_{in}\hat{c}_{k\sigma}\rangle$ and of the self-energies quantities $\Xi(\omega)$ introduced in Eq. (17) are given in the Appendix. In all the expressions above $\omega \equiv (\omega - i\eta)_{\eta\to 0}$, because of the advanced Green's functions used [Eq. (14)].

Equation (17) relates the Green's function $G_{A^1_{ij}}(\hat{A}^{(1)}_{qm})$ to other components such as $G_{A^1_{ij}}(\hat{A}^{(1)}_{qp})$, $G_{A^1_{ij}}(\hat{A}^{(2)}_{pl})$, $G_{A^1_{ij}}(\hat{B}^{(1)}_{np})$, and $G_{A^1_{ij}}(\hat{B}^{(2)}_{lp})$; these off-diagonal terms are second order compared with the original Green's function, $G_{A^1_{ij}}(\hat{A}^{(1)}_{qm})$, and one is tempted to neglect them for calculating the original one. This is what we did in Ref. [35] to calculate the properties of the Fe-Co dimer. However, we have checked that this is a bad approximation for calculating the Co-Co dimer, the reason being the degenerate states that one finds around the Fermi energy in the atomic Hamiltonian (10). In Ref. [35] we also neglected in Eq. (18) the last two terms; both are important when analyzing the Co-Co case. In particular, the term like $1/(\omega - \varepsilon_k - E_n^{S,s-1/2} + E_m^{S-1/2,s})$ is associated with the transfer of an excitation in one atom to the other; its contribution is important for the Co-Co case because $(-E_n^{S,s-1/2} + E_m^{S-1/2,s})$ can be zero for this case.

We should comment that, although the EOM equations are solved up to second order in the atom-surface coupling ($T^{\alpha}T^{\beta *}$), the Green's functions, as calculated in Eqs. (17) and (18), go to a higher order, as can be easily checked by realizing that those second-order terms appear in $g_0^{-1}(\hat{Z}_{qm}^{(\alpha)})$ [Eq. (18)]. Notice that the one-electron problem for an atom-surface interaction, without many-body effects, can be calculated exactly by using the second-order EOM method.

On the other hand, it is interesting to realize that the different self-energy terms of Eqs. (17) and (18) are proportional to either $(T^A T^{A*})$, $(T^B T^{B*})$, $(T^A T^{B*})$, or $(T^B T^{A*})$. The last two factors, $(T^A T^{B*})$ or $(T^B T^{A*})$, are proportional to $\exp(\pm i\vec{k}\cdot\vec{R})$, $\vec{R}$ being the vector joining atoms A and B. Then, notice that for $\Sigma_k \exp(\pm i\vec{k}\cdot\vec{R})$, the angular integration yields (taking k constant and assuming the energy band to be spherically symmetric) the following factor:$\sin(kR)/kR$. For the Cu Fermi energy, $k_F = 1.36/A$, so that for the expected distances of $R > 2A$ we find $|\sin(k_F R)/k_F R| < 0.2$, indicating that the terms with the off-diagonal contributions, $(T^A T^{B*})$ or $(T^B T^{A*})$, should be much smaller than the diagonal ones, $(T^A T^{A*})$ or $(T^B T^{B*})$. As discussed below, calculations with $(T^A T^{B*})$ and $(T^B T^{A*})$ smaller than $0.2|T^A|^2$ and $0.2|T^B|^2$ yield results similar to taking $(T^A T^{B*}) = (T^B T^{A*}) = 0$; therefore, we are going to assume this condition to be satisfied in most of the cases presented in this paper. Notice that in this limit the atoms see each other only through the interaction $J\vec{S}\div\vec{s}$, in such a way that for $J = 0$ one should recover the case of independent atoms; this suggests to approximate Eqs. (17) and (18) by including spin fluctuations in atom A, and neglecting contributions from spin fluctuations in atom B that is assumed to keep its spin s. This approximation reduces Eqs. (17) and (18) to the following expression:

$$\left[\omega - E_q^{S,s} + E_m^{S-1/2,s} - \sum_{k,\sigma,n} \frac{\left|T^{A^1}_{k,\sigma,n,q}\right|^2 \langle 1-n_{k\sigma}\rangle}{\omega-\varepsilon_k-E_n^{S-1/2,s}+E_m^{S-1/2,s}} - \sum_{k,\sigma,n} \frac{\left|T^{A^1}_{k,\sigma,m,n}\right|^2 \langle n_{k\sigma}\rangle}{\omega-\varepsilon_k-E_q^{S,s}+E_n^{S,s}}\right] G_{A^1_{ij}}\left(\hat{A}^{(1)}_{qm}\right)$$

$$= \left\langle \left|\psi_q^{S,s}\right\rangle\left\langle\psi_i^{S,s}\right|\delta_{jm} + \left|\psi_j^{S-1/2,s}\right\rangle\left\langle\psi_m^{S-1/2,s}\right|\delta_{iq}\right\rangle + \sum_{k,\sigma,n} \frac{T^{A^1}_{k\sigma nq}\left\langle \hat{A}^{(1)\dagger}_{in}\hat{c}_{k\sigma}\right\rangle}{\omega-\varepsilon_k-E_n^{S-1/2,s}+E_j^{S-1/2,s}}\delta_{jm}$$

$$- \sum_{k,\sigma,p} \frac{T^{A^1}_{k\sigma mp}\left\langle \hat{A}^{(1)\dagger}_{pj}\hat{c}_{k\sigma}\right\rangle}{\omega-\varepsilon_k-E_i^{S,s}+E_p^{S,s}}\delta_{qi} + \sum_{p\neq m} \Xi^{A^1(\mathrm{I})}_{qp}(\omega) G_{A^1_{ij}}\left(\hat{A}^{(1)}_{qp}\right) + \sum_{p\neq q} \Xi^{A^1(\mathrm{II})}_{pm}(\omega) G_{A^1_{ij}}\left(\hat{A}^{(1)}_{pm}\right). \tag{19}$$

In this approximation, the information about the magnetocrystalline field and the exchange interaction between atoms is only introduced in the calculation of the eigenvalues and eigenstates of the corresponding atomic Hamiltonian. Equation (19) will be used in some specific cases to be discussed below; a further approximation to Eq. (19) will be introduced by neglecting the off-diagonal Green's functions, $G_{A^1_{ij}}(\hat{A}^{(1)}_{qm})$.

V. THE TUNNELING CURRENT

The tunneling current, when the tip is positioned simultaneously over the two atoms (A) and (B), is calculated as $I_A^{\sigma} + I_B^{\sigma} = -\frac{e}{\hbar}\sum_{k_t} d\langle\hat{n}_{k_t\sigma}\rangle/dt$; this equation takes into account the transfer processes between the $k_t\sigma$ electrons of the tip and the magnetic atoms (we are now discriminating k into the two possibilities, k_t for the tip and k_S for the surface). A direct calculation of $[\hat{n}_{k_t\sigma}, \hat{H}]$ leads to the expression for I_Z^{σ} $(Z = A, B)$:

$$I_Z^{\sigma} = -\frac{2e}{\hbar}\mathrm{Im}\left[\sum_{k_t,i,j} T^{Z^1 *}_{k_t\sigma ji}\left\langle \hat{Z}^{(1)\dagger}_{ij}\hat{c}_{k_t\sigma}\right\rangle + \sum_{k_t,i,j} T^{Z^2 *}_{k_t\sigma ji}\left\langle \hat{Z}^{(2)\dagger}_{ij}\hat{c}_{k_t\sigma}\right\rangle\right]. \tag{20}$$

Following the same procedure as that in Ref. [34], the conductance $G = dI/dV$, measured with the tip over the atom A in the limit of low temperatures and small bias voltages V, but considering the interference terms due to the possibility of the tip seeing the atom B too, is given by (G_0 is the quantum of conductance)

$$G_A/G_0 = \sum_{\sigma ijqm} \Gamma(A^1A^1)_{ijqm}\mathrm{Im}G_{A^1_{ij}}\left(\hat{A}^{(1)}_{qm}\right) + \sum_{\sigma ijqm} \Gamma(A^1A^2)_{ijqm}\mathrm{Im}G_{A^1_{ij}}\left(\hat{A}^{(2)}_{qm}\right)$$

$$+(-1)^{2S}\sum_{\sigma ijqm} \Gamma(A^1B^1)_{ijqm}\mathrm{Im}G_{A^1_{ij}}\left(\hat{B}^{(1)}_{qm}\right) + (-1)^{2S-1}\sum_{\sigma ijqm} \Gamma(A^1B^2)_{ijqm}\mathrm{Im}G_{A^1_{ij}}\left(\hat{B}^{(2)}_{qm}\right)$$

$$+ \sum_{\sigma ijqm} \Gamma(A^2A^1)_{ijqm}\mathrm{Im}G_{A^2_{ij}}\left(\hat{A}^{(1)}_{qm}\right) + \sum_{\sigma ijqm} \Gamma(A^2A^2)_{ijqm}\mathrm{Im}G_{A^2_{ij}}\left(\hat{A}^{(2)}_{qm}\right)$$

$$+(-1)^{2S}\sum_{\sigma ijqm} \Gamma(A^2B^1)_{ijqm}\mathrm{Im}G_{A^2_{ij}}\left(\hat{B}^{(1)}_{qm}\right) + (-1)^{2S-1}\sum_{\sigma ijqm} \Gamma(A^2B^2)_{ijqm}\mathrm{Im}G_{A^2_{ij}}\left(\hat{B}^{(2)}_{qm}\right). \tag{21}$$

The quantities Γ in Eq. (21) define an effective broadening given by

$$\Gamma(A^{\alpha}Z^{\beta})_{ijqm} = 2\Gamma^{A^{\alpha}Z^{\beta}}_{\sigma jimq(tip)}, \tag{22a}$$

where

$$\Gamma^{A^{\alpha}Z^{\beta}}_{\sigma jimq(tip)}(\varepsilon) = \pi \sum_{k_t} T^{A^{\alpha}*}_{k_t\sigma ji} T^{Z^{\beta}}_{k_t\sigma mq} \delta(\varepsilon - \varepsilon_{k_t}). \tag{22b}$$

Notice that Eq. (21) has the conventional form of a tunneling current [44,45]: the terms like ImG are associated with the density of states of the magnetic atom in its interaction with the metal (because the tip-atom interaction is negligible), in such a way that the tunneling current is proportional to that density of states and to a factor like $\Gamma(Z_1Z_2) = \pi T_t^{Z_1*} T_t^{Z_2} \rho_t(\varepsilon)$, which includes the tip density of states and a second-order term (T^2) in the tip-atom interaction.

If $Z = B$ in Eq. (22b), we find a contribution like $\Sigma_k V_k{}^{A*} V_k{}^{B}$, which is small for the reasons given above. Neglecting these contributions, we find, for the conductance measured in atom A, the simplified expression:

$$\begin{aligned} G_A/G_0 = 4 \sum_{ijqm} & \Gamma^{A^1A^1}_{jimq(tip)} \mathrm{Im}G_{A^1_{ij}}\left(\hat{A}^{(1)}_{qm}\right) \\ & + 4 \sum_{ijqm} \Gamma^{A^1A^2}_{jimq(tip)} \mathrm{Im}G_{A^1_{ij}}\left(\hat{A}^{(2)}_{qm}\right) \\ & + 4 \sum_{ijqm} \Gamma^{A^2A^1}_{jimq(tip)} \mathrm{Im}G_{A^2_{ij}}\left(\hat{A}^{(1)}_{qm}\right) \\ & + 4 \sum_{ijqm} \Gamma^{A^2A^2}_{jimq(tip)} \mathrm{Im}G_{A^2_{ij}}\left(\hat{A}^{(2)}_{qm}\right). \end{aligned} \tag{23}$$

And in the case of neglecting the fluctuations in atom A in the presence of atom B with spin s-1/2, the conductance reduces to the first term of Eq. (23).

VI. TWO ATOMS WITH SPIN $s = S = 1/2$

In this section we analyze the conductance for a symmetric dimer with $S = s = 1/2$; this simple case will allow us to compare the complete description provided by Eq. (18) with other simplifications discussed above [see Eq. (19) and the ensuing discussion].

As mentioned above, we consider an interaction between the two atoms provided by a Heisenberg term $J\hat{S}\cdot\hat{s}$, in such a way that positive (negative) values of the exchange parameter J mean an antiferromagnetic (ferromagnetic) interaction between atomic spins.

In the case of a dimer formed by atoms with equal spin, we will suppress the total spin of each atom in the notation $|SM,sm\rangle$. Then, different configurations will be denoted by $|\sigma,\sigma'\rangle, |\sigma,0\rangle, |0,\sigma'\rangle$ and $|0,0\rangle$.

When the Heisenberg interaction between atoms is turned on, we have the triplet state with total spin 1:

$$\psi_1^{1/2,1/2} = \frac{1}{\sqrt{2}}[|\uparrow,\downarrow\rangle + |\downarrow,\uparrow\rangle];$$
$$\psi_2^{1/2,1/2} = |\uparrow,\uparrow\rangle; \quad \psi_3^{1/2,1/2} = |\downarrow,\downarrow\rangle$$

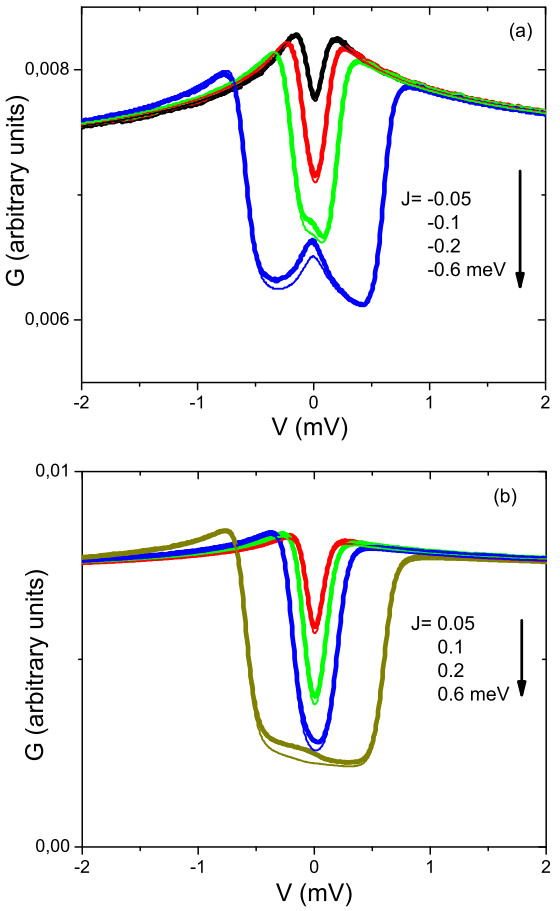

FIG. 1. The complete calculation [Eq. (17)] for the 1/2-1/2 dimer. The thin lines correspond to the conductance neglecting the crossed interaction term ($\Gamma^{AB}_{(\mathrm{surface})} = 0$) and the thick lines to the conductance calculated by considering $\Gamma^{AB}_{(\mathrm{surface})} = 0.2\Gamma^{AA}_{(\mathrm{surface})}$, for several values of the exchange interaction between atoms, J. (a) Ferromagnetic interaction. (b) Antiferromagnetic interaction ($\varepsilon_d = 1$ eV and $\Gamma^{AA}_{(\mathrm{surface})} = 0.05$ eV).

with energy $E^{1/2,1/2}_{1,2,3} = 2\varepsilon_d + (1/4)J$, and the singlet, $\psi_4^{1/2,1/2} = \frac{1}{\sqrt{2}}[|\uparrow,\downarrow\rangle - |\downarrow,\uparrow\rangle]$ with energy $E_4^{1/2,1/2} = 2\varepsilon_d - (3/4)J$. Obviously, for $J < 0$ (> 0) the ground state is a triplet (singlet). In these equations, $2\varepsilon_d$ is the energy of the two electrons for the noninteracting atoms.

The other spin dimer configurations involving spin fluctuation in one atom are $\psi_1^{0,1/2} = |0,\uparrow\rangle$; $\psi_2^{0,1/2} = |0,\downarrow\rangle$; $\psi_3^{1/2,0} = |\uparrow,0\rangle$ and $\psi_4^{1/2,0} = |\downarrow,0\rangle$ with energy ε_d; finally, the configuration $\psi_1^{0,0} = |0,0\rangle$ corresponds to having spin fluctuations in both atoms.

The results we are going to show correspond to $\varepsilon_d = 1$ eV and two possible values of $\Gamma^{AA}_{(\mathrm{surface})}$ [Eq. (22c)]: 0.05 and 0.1 eV. We consider first the cases for which $\Gamma^{AB} = 0$ or $\Gamma^{AB} = 0.2\Gamma^{AA}$, and calculate the differential conductance across the atom A using the first term of Eq. (24) and $\Gamma^{AA}_{(\mathrm{surface})} = 0.05$ eV. Comparing both cases in Fig. 1, we see that $\Gamma^{AB}_{(\mathrm{surface})} = 0.2\Gamma^{AA}_{(\mathrm{surface})}$ yields a differential conductance very close to that calculated for $\Gamma^{AB}_{(\mathrm{surface})} = 0$. This result substantiates our claim that the Γ^{AB} interaction, for $\Gamma^{AB}_{(\mathrm{surface})} <$

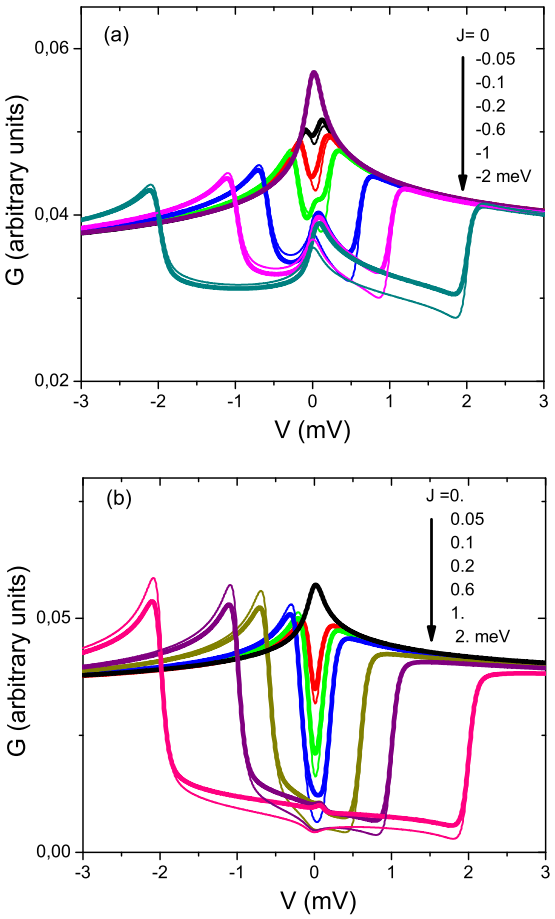

FIG. 2. The 1/2-1/2 dimer case taking the crossed interaction term $\Gamma^{AB}_{(\text{surface})} = 0$. Complete version, Eq. (17), (thick lines) compared with the approximated version, Eq. (19), (thin lines); $\Gamma^{AA}_{(\text{surface})} = 0.1$ eV. (a) Ferromagnetic interaction. (b) Antiferromagnetic interaction.

$0.2\Gamma^{AA}_{(\text{surface})}$, has a very small effect on the conductance; therefore, we are going to assume from now on for all the calculations presented in this paper that $\Gamma^{AB}_{(\text{surface})} = 0$; we stress, however, that this assumption does not imply that J, in $J\hat{S}\cdot\hat{s}$, proportional to $|V_k{}^A|^2|V_k{}^B|^2$, is also negligible, because even if J is small it has an important effect on the degeneracy of the levels around the Fermi energy, degeneracy that is associated with the fine structure located for the differential conductance around that Fermi level. We should also comment that the case $\Gamma^{AB} = \Gamma^{AA} = \Gamma^{BB}$ (not discussed here in detail) decouples the singlet and the triplet states of the 1/2-1/2 dimer, in such a way that its differential conductance spectrum only shows a kind of Kondo resonance at the Fermi energy [46].

In particular, the conductance steps, located at around $\pm J$ in Figs. 1(a) and 1(b), are associated with the excitations between the singlet and triplet states.

In Fig. 2 we compare the conductance calculated by using Eq. (24) for (a) the Green's functions obtained from Eqs. (17) and (18) (complete version), and (b) the Green's functions given by Eq. (19) (approximate version). Figure 2(a) corresponds to a ferromagnetic interaction ($J = -0.05, -0.1, -0.2, -0.6, -1$, and -2 meV) and Fig. 2(b) to an antiferromagnetic one ($J = 0.05, 0.1, 0.2, 0.6, 1$, and 2 meV).

The first thing to notice is that both solutions are very close to each other for small values of Γ and J; only for the largest values of Γ and J some small discrepancies between both solutions appear. On the other hand, regarding the general properties of the results shown in Fig. 2, notice the following points: (a) the solution for $J = 0$ shows a Kondo peak that corresponds to the case of an isolated atom, because in this limit there is no interaction between the two atoms. (b) For the ferromagnetic case, that Kondo peak evolves into a dip around the Fermi energy as J increases, but for large values of J (between 0.5 and 2 meV) a new Kondo resonance appears associated with the degeneracy of the triplet ground state. Moreover, the solution also shows the conductance steps associated with the excitations between the triplet and the singlet states. (c) For the antiferromagnetic case, the Kondo resonance found for $J = 0$ evolves, for large values of J, into a single dip between the conductance steps associated with the singlet-triplet excitation. We should stress that for both the antiferromagnetic and the ferromagnetic cases the Kondo peak appearing for $J \to 0$ disappears for very small values of J, namely, as far as the triplet-singlet splitting is larger than the Kondo resonance width. This indicates that there are channels mixing the singlet and triplet states that are crucial in the destruction of the Kondo state.

We conclude from these calculations that taking $\Gamma^{AB} = 0$ is a good approximation to our general solution, and that Eq. (19) represents a fair approximation to Eqs. (17) and (18).

VII. A SIMPLE APPROXIMATION TO THE Co/Co case

We start analyzing this dimer by taking the minimum basis set that allows us to describe within a reasonable approximation the tunneling current around the Fermi energy. In this approximation we consider Hamiltonian (8) for a Co atom ($S = 3/2$) with $D = 2.8$ meV and $E = 0$ [8], and realize that its eigenstates and eigenvalues are $|3/2, \pm 3/2\rangle$, $E^{3/2,\pm 3/2} = 9D/4$ and $|3/2, \pm 1/2\rangle$, $E^{3/2,\pm 1/2} = D/4$; as $E^{3/2,\pm 3/2} - E^{3/2,\pm 1/2} = 2D$ (5.4 meV) we neglect the $|3/2, \pm 3/2\rangle$ levels and consider only the $|3/2, \pm 1/2\rangle$ states in this approximation, valid only for energies close to the Fermi level (<3 meV). This implies that the Co/Co dimer is analyzed by means of the following four states: $|3/2, \pm 1/2; 3/2, \pm 1/2\rangle$, which is reminiscent of the 1/2-1/2 case discussed above. As in this case, we introduce the triplet and singlet states and use a similar notation, so that

$$\Psi_1{}^{1/2,1/2}(S = 3/2) = 1/\sqrt{2}[|\uparrow,\downarrow\rangle + |\downarrow,\uparrow\rangle];$$
$$\Psi_2{}^{1/2,1/2}(S = 3/2) = |\uparrow,\uparrow\rangle;$$
$$\Psi_3{}^{1/2,1/2}(S = 3/2) = |\downarrow,\downarrow\rangle;$$
$$\text{and } \Psi_4{}^{1/2,1/2}(S = 3/2) = 1/\sqrt{2}[|\uparrow,\downarrow\rangle - |\downarrow,\uparrow\rangle];$$

the corresponding energies associated with $J\hat{S}_1\cdot\hat{S}_2$ are

$$E_1{}^{1/2,1/2}(S = 3/2) = 7J/4; \quad E_2{}^{1/2,1/2}(S = 3/2) = J/4;$$
$$E_3{}^{1/2,1/2}(S = 3/2) = J/4; \quad \text{and}$$
$$E_4{}^{1/2,1/2}(S = 3/2) = -9J/4;$$

notice that the energies E_2 and E_3 are the same as before, but E_1 and E_4 are different due to the matrix element

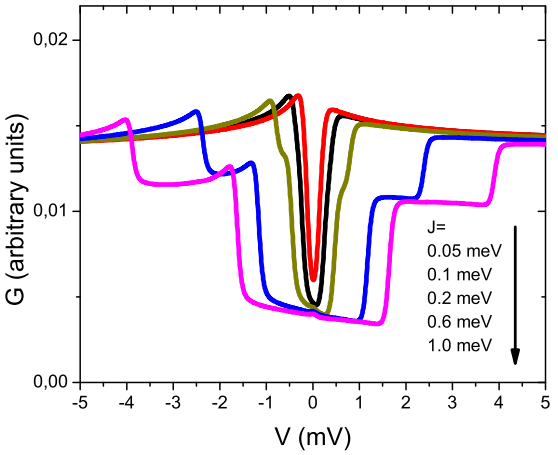

FIG. 3. The conductance spectra for a simplified Co dimer in the case of an antiferromagnetic interaction for the J values indicated in the figure and the same energy level and width parameters of Fig. 2 ($\Gamma^{AA}_{(\text{surface})} = 0.1$ eV and $\varepsilon_d = 1$ eV).

$\langle\uparrow,\downarrow|J\hat{S}_1\cdot\hat{S}_2|\downarrow,\uparrow\rangle$ that changes because we are now working in the 3/2-spin space.

As the Co atoms with spin 3/2 jump to the states having spin 1, we have to consider the different states $|1,1\rangle$; $|1,0\rangle$ and $|1,-1\rangle$ for each atom; however, Hamiltonian (8) locates states $|1,1\rangle$ and $|1,-1\rangle$, 2.8 meV above the $|1,0\rangle$ state. Consistently with the previous approximation for $S = 3/2$, we only keep the state $|1,0\rangle$ for $S = 1$, and work in the $S = 3/2^*S = 1$ or the $S = 1^*S = 3/2$ space with the states

$$|1/2;0\rangle;|-1/2;0\rangle \text{ and } |0;1/2\rangle;|0;-1/2\rangle,$$

where components $|0\rangle$ and $|\pm 1/2\rangle$ refer to the $|S = 1,0\rangle$ and the $|S = 3/2,\pm 1/2\rangle$ states.

Finally, if both atoms jump from $S = 3/2$ to $S = 1$, we work in the $S = 1^*S = 1$ space and consider only, in consistency with previous approximations, the state ($S = 1, m = 0; S = 1, m = 0$) which we represent by $|0;0\rangle$.

It is interesting to realize that this approximation for the Co/Co dimer yields a similar Hamiltonian to that discussed above for the 1/2-1/2-case; the only difference appears in the energies of the states ${\Psi_i}^{1/2,1/2}$, because we now have the triplet states ${\Psi_2}^{1/2,1/2}$ and ${\Psi_3}^{1/2,1/2}$ degenerate but different from the other triplet state ${\Psi_1}^{1/2,1/2}$: ${E_1}^{1/2,1/2}(S = 3/2) - {E_2}^{1/2,1/2}(S = 3/2) = 3J/2$; moreover, ${E_2}^{1/2,1/2}(S = 3/2) - {E_4}^{1/2,1/2}(S = 3/2) = 5J/2$.

These results show how the doublet associated with the individual Co atoms is broken by the $J\hat{S}_1\cdot\hat{S}_2$ interaction.

In Fig. 3 we show the differential conductance behavior around the Fermi level in the case of an antiferromagnetic interaction between the Co atoms, calculated using the simplified model described before. When compared with the same calculation for the dimer of atoms with spin 1/2 [Fig. 2(b)], we observe that the steps associated to the excited states in the Co dimer begin to be visible at J values larger than 0.1/meV; this indicates that to model the Co-Co system as a typical spin-½ system does not reproduce the correct structure of the conductance spectra for relatively large values of J.

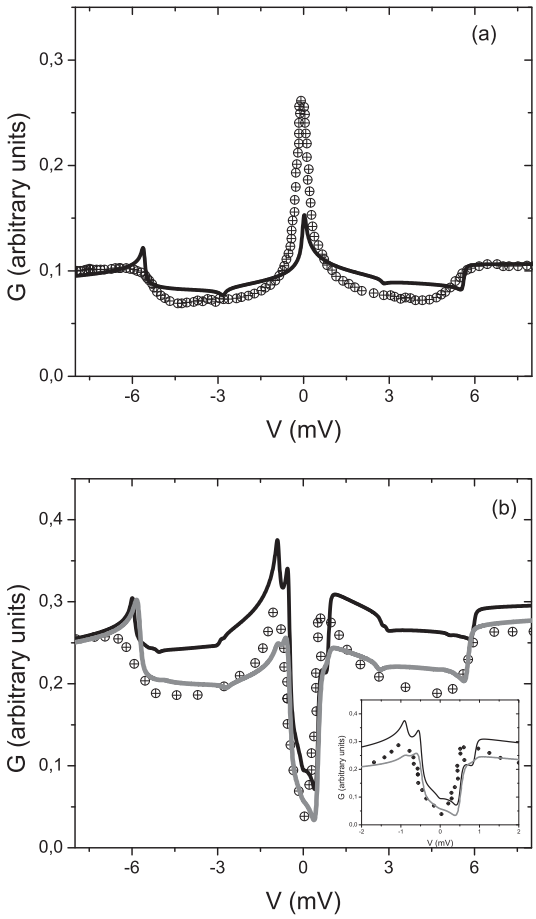

FIG. 4. Conductance through a Co atom as a function of the applied voltage for zero magnetic field. Isolated Co atom: the calculated results (solid line) and the experimental results (crossed circles). The theoretical results considering $J = 0.22$ meV for Co-Co dimer (0,2) of Ref. [13]: black solid line corresponds to the calculation including only the diagonal Green's function components $G_{A^1_{ij}}(\hat{A}^{(1)}_{ij})$; gray solid line corresponds to the calculation including diagonals and nondiagonals $G_{A^1_{ij}}(\hat{A}^{(1)}_{pq})$ but within a reduced space of (10,4,4,1) states. The crossed circles are the experimental results [13]. The inset is a zoom of the calculated conductance behavior close to zero energy.

VIII. GENERAL CALCULATIONS FOR Co-Co AND Fe-Fe DIMERS

A. Co-Co dimer

We analyze this case in several steps. First, we calculate the case of a single Co atom: as discussed in Ref. [34], in this case we use Eq. (19) by neglecting all the off-diagonal Green's functions and keeping only the diagonal components $G_{A^1_{ij}}(\hat{A}^{(1)}_{ij})$. We find for this single atom that the experimental curve is well fitted [see Fig. 4(a)] by using a level width $\Gamma^{AA}_{(\text{surface})} = 200$ meV; this quantity and the phenomenological anisotropy parameters $D = 0.28$ meV, $E = 0$ [2] were used in this calculation and in all the others presented below.

For the Co dimer we have calculated the differential conductance, and compared with the experimental results of Ref. [13] for the dimer (0,2), using two different approximations since a complete calculation with all the diagonal and off-diagonal

Green's functions goes beyond our computational capabilities: (i) we consider the complete configurational $A_{ij}^{(1)}$ space, but including only the diagonal Green's function components $G_{A_{ij}^1}(\hat{A}_{ij}^{(1)})$, and (ii) also considering the configurational $A_{ij}^{(1)}$ space but including both the diagonal and off- diagonal Green's function components, within a reduced space including only the ten lowest energy configurations for spins (S, s), the four lowest ones for spins (S, s-1/2) or (S-1/2,s), and the lowest one for (S-1/2,s-1/2). This calculation, which we will refer to as (10,4,4,1), provides a better description of the conductance spectra for $J = 0.22$ meV in the energy region around the Fermi energy [see Fig. 4(b)].

Notice that for the isolated atom the agreement between the theoretical calculation and the experimental data [Fig. 4(a)] is good except near the Fermi energy, because our approximation does not reproduce with good accuracy the Kondo resonance [34]. On the other hand, our results for the Co-Co case and the (10,4,4,1) approximation [Fig. 4(b)] are in very good agreement with the experimental data around the Fermi energy, although a small discrepancy appears for $V = 3-5$ meV; in the inset of this figure we can observe the conductance steps at $(5/2)J$ and $4J$ associated with the broken degeneration for an antiferromagnetic interaction of the quadruplet states of the isolated Co atoms (as already found for the simple case discussed in Sec. VII). The results calculated using only the diagonal Green's function components $G_{A_{ij}^1}(\hat{A}_{ij}^{(1)})$ are only reasonable even if they reproduce the main characteristics of the experiments.

Notice also in Fig. 4, some kinks in the spectra around ± 3 meV; they are associated with the term $\Sigma_k T^2\langle 1-\hat{n}_k\rangle/(\omega-\varepsilon_k-E_n^{S-1/2,s}+E_m^{S-1/2,s})$ and the condition $\omega = E_n^{S-1/2,s} - E_m^{S-1/2,s}$. In other words, the kink is due to the excited states in the magnetic atom for $S = 1$; as discussed above in Sec. VII, the energy difference between the degenerate states $|1,1\rangle$ and $|1,-1\rangle$ and the state $|1,0\rangle$, is 2.8 meV, in perfect agreement with the energy position of the observed kink.

In the following figure we examine the behavior of the conductance vs applied voltage, when there is a magnetic field applied in the x direction (Fig. 5). Both calculations use the same parameters as in Fig. 4, and are compared with the experimental data for 4 and 8 T.

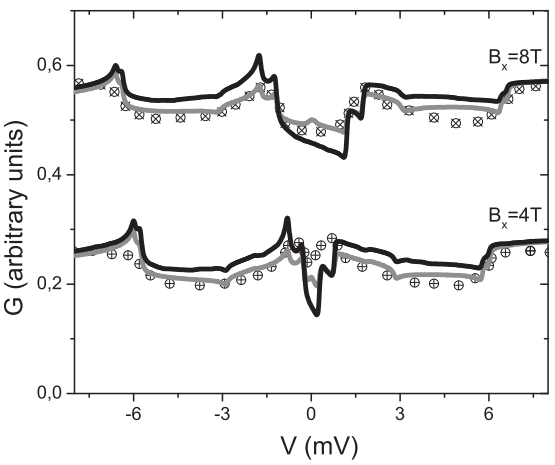

FIG. 5. The same as in Fig. 4 for a magnetic field applied in the x direction. The symbols are the experimental results of Ref. [13].

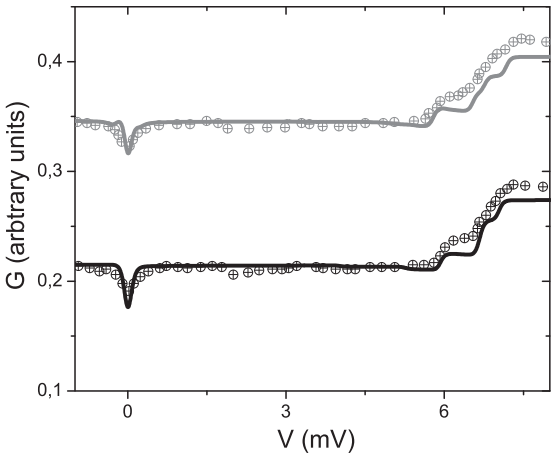

FIG. 6. Theory (lines) vs experiment (symbols) for the Fe-Fe dimer in the geometry (2,0) of Ref. [14]. In absence of a magnetic field (black curves) and in the presence of a magnetic field in the z direction $B_z = 2$ T (gray curves).

Our theoretical results are again in very good agreement with the experiments for $B = 8$ T and the (10,4,4,1) approximation; the jumps in the differential conductance are related to the excited eigenstates of the atomic Hamiltonian. For $B = 4$ T, our results are not so good; this is probably related to the Kondo resonance that appears in this problem for a magnetic field of 3.1 T [13]; this Kondo resonance effect makes the dip near the Fermi energy too deep in our theoretical calculation, although the (10,4,4,1) approximation seems to be in better agreement with the experimental data.

B. Fe-Fe dimer

In the case of two Fe atoms, where the ground state is a singlet state in any case, for interacting or noninteracting atoms, the conductance spectra only show a rather smooth structure less rich around the Fermi energy than the one found for the Co-Co case, due to the smaller number of atomic excitations found in this case. In Fig. 6 we can observe that the simplest calculation (i) which considers the complete configurational $A_{ij}^{(1)}$ space, but including only the diagonal Green's function components $G_{A_{ij}^1}(\hat{A}_{ij}^{(1)})$, reproduces adequately the experimental results for the dimer (2,0) of Ref. [14], which corresponds to an antiferromagnetic interaction $J = 0.7$ meV either for zero magnetic field or for $B = 2$ T. In our calculations we use the anisotropy parameters $D = -1.87$ meV and $E = 0.31$ meV of Ref. [9], and a level width $\Gamma^{AA}_{(\text{surface})} = 160$ meV [29].

IX. CONCLUSIONS

In this paper we have presented an analysis of the differential conductance across the Co/Co and Fe/Fe dimers deposited on a metal surface. Our approach is based on the analysis of an Anderson Hamiltonian which is introduced following these steps: (i) First, we introduce an ionic Hamiltonian

describing the electron charge transfer between the atom and the metal assuming that, due to the low symmetry of the atom environment, the ground state of the magnetic atom is an orbital singlet. (ii) In a second step, this Hamiltonian is extended to a dimer configuration including also an anisotropy term and a Zeeman energy. (iii) That basic Hamiltonian for the dimer is solved calculating some appropriate Green's functions using an equation of motion method. (iv) In a final step, the differential conductance across the dimer is calculated in terms of the Green's functions provided by the equation of motion method.

Then, we apply that formalism to the ideal 1/2-1/2 dimer, a case that presents interesting similarities and differences with a simplified Co/Co model; the main difference between these two cases comes from the different excited states the systems have around the Fermi energy. Finally, we consider the full Co/Co and Fe/Fe cases; our results for these dimers show a good agreement with the experimental evidence. We only find some discrepancies with the experiments when a Kondo resonance appears in the problem; in those cases, our calculations based on the EOM solution are not good enough to collect the subtleties of the problem, otherwise our theoretical differential conductance reproduces well the experimental data and the electron excitations of the magnetic atom.

ACKNOWLEDGMENTS

E.C.G. acknowledges financial support by CONICET through Grant No. PIP-112201-50100546CO and U.N.L. through CAI+D grants. F.F. acknowledges support from the Spanish Ministerio de Economía y Competitividad (MINECO) under project MAT2014-59966-R and through the "María de Maeztu" Programme for Units of Excellence in R&D (MDM-2014-0377).

APPENDIX

The self-energies introduced in Eqs. (17) and (18) have the following expressions:

$$
\begin{aligned}
\Xi^{A^1(\mathrm{I})}_{qp}(\omega) &= \sum_{k,\sigma}\left[\sum_n \frac{T^{A^1}_{k\sigma mn}T^{A^1}_{k\sigma pn}\langle \hat{n}_{k\sigma}\rangle}{\omega-\varepsilon_k-E^{S,s}_q+E^{S,s}_n}+\sum_l \frac{T^{B^2}_{k\sigma lm}T^{B^2}_{k\sigma lp}\langle 1-\hat{n}_{k\sigma}\rangle}{\omega+\varepsilon_k-E^{S,s}_q+E^{S-1/2,s-1/2}_l}\right],\\
\Xi^{A^1(\mathrm{II})}_{pm}(\omega) &= \sum_{k,\sigma}\left[\sum_n \frac{T^{*B^1}_{k\sigma nq}T^{B^1}_{k\sigma np}\langle 1-\hat{n}_{k\sigma}\rangle}{\omega-\varepsilon_k-E^{S,s-1/2}_n+E^{S-1/2,s}_m}+\sum_n \frac{T^{*A^1}_{k\sigma nq}T^{A^1}_{k\sigma np}\langle 1-\hat{n}_{k\sigma}\rangle}{\omega-\varepsilon_k-E^{S-1/2,s}_n+E^{S-1/2,s}_m}\right],\\
\Xi^{A^2}_{pl}(\omega) &= \sum_{k,\sigma}T^{B^1}_{k\sigma pq}\langle \hat{n}_{k\sigma}\rangle\left[\frac{T^{B^2}_{k\sigma lm}}{\omega-\varepsilon_k-E^{S,s-1/2}_p+E^{S-1/2,s}_m}+\frac{T^{B^2}_{k\sigma lm}}{\omega+\varepsilon_k-E^{S,s}_q+E^{S-1/2,s-1/2}_l}\right],\\
\Xi^{B^1}_{qp}(\omega) &= \sum_{k,\sigma}\left[\sum_l \frac{T^{A^1}_{k\sigma ml}T^{B^1}_{k\sigma pl}\langle \hat{n}_{k\sigma}\rangle}{\omega-\varepsilon_k-E^{S,s}_q+E^{S,s}_l}-\sum_n \frac{T^{A^2}_{k\sigma np}T^{B^2}_{k\sigma nm}\langle 1-\hat{n}_{k\sigma}\rangle}{\omega+\varepsilon_k-E^{S,s}_q+E^{S-1/2,s-1/2}_n}\right],\\
\Xi^{B^2}_{lp}(\omega) &= \sum_{k,\sigma}T^{A^1}_{k\sigma lq}\langle \hat{n}_{k\sigma}\rangle\left[\frac{T^{B^2}_{k\sigma pm}}{\omega-\varepsilon_k-E^{S-1/2,s}_l+E^{S-1/2,s}_m}+\frac{T^{B^2}_{k\sigma pl}}{\omega+\varepsilon_k-E^{S,s}_q+E^{S-1/2,s-1/2}_p}\right].
\end{aligned}
\tag{A1}
$$

The atom-band crossed terms needed for calculating the Green's functions [see Eq. (17)] are calculated in terms of them in the equilibrium condition:

$$
\begin{aligned}
\langle \hat{A}^{(1)\dagger}_{in}\hat{c}_{k\sigma}\rangle &= \sum_{l,p}T^{A^1}_{k\sigma lp}\frac{\mathrm{Im}}{\pi}\int_{-\infty}^{\infty}d\omega'\frac{G_{\hat{A}^{(1)}_{in}}\left(\hat{A}^{(1)}_{pl}\right)}{\omega'-\omega}+\sum_{l,p}T^{A^2}_{k\sigma lp}\frac{\mathrm{Im}}{\pi}\int_{-\infty}^{\infty}d\omega'\frac{G_{\hat{A}^{(1)}_{in}}\left(\hat{A}^{(2)}_{pl}\right)}{\omega'-\omega}\\
&+(-1)^{2S}\sum_{l,p}T^{B^1}_{k\sigma lp}\frac{\mathrm{Im}}{\pi}\int_{-\infty}^{\infty}d\omega'\frac{G_{\hat{A}^{(1)}_{in}}\left(\hat{B}^{(1)}_{pl}\right)}{\omega'-\omega}+(-1)^{2(S-1/2)}\sum_{l,p}T^{B^2}_{k\sigma lp}\frac{\mathrm{Im}}{\pi}\int_{-\infty}^{\infty}d\omega'\frac{G_{\hat{A}^{(1)}_{in}}\left(\hat{B}^{(2)}_{pl}\right)}{\omega'-\omega}.
\end{aligned}
\tag{A2}
$$

[1] C. F. Hirjibehedin, C. P. Lutz, and A. J. Heinrich, Science **312**, 1021 (2006).

[2] C. F. Hirjibehedin, C. Y. Lin, A. F. Otte, M. Ternes, C. P. Lutz, B. A. Jones, and A. J. Heinrich, Science **317**, 1199 (2007).

[3] A. F. Otte, M. Ternes, S. Loth, K. von Bergmann, H. Brune, C. P. Lutz, C. F. Hirjibehedin, and A. J. Heinrich, Nat. Phys. **4**, 847 (2008).

[4] M. Ternes, A. J. Heinrich, and W. D. Schneider, J. Phys.: Condens. Matter **21**, 053001 (2009).

[5] A. J. Heinrich, J. A. Gupta, C. P. Lutz, and D. M. Eigler, Science **306**, 466 (2004).

[6] A. C. Hewson, *The Kondo Problem to Heavy Fermions* (Cambridge University Press, Cambridge, 1993).

[7] F. Flores and E. C. Goldberg, J. Phys.: Condens. Matter **29**, 055602 (2017).

[8] R. Bulla, T. A. Costi, and T. Pruschke, Rev. Mod. Phys. **80**, 395 (2008).

[9] J. J. Parks *et al.*, Science **328**, 1370 (2010).

[10] F. Delgado, S. Loth, M. Zielinski, and J. Fernandez-Rossier, Europhys. Lett. **109**, 57001 (2015).
[11] A. A. Khajetoorians *et al.*, Science, **339**, 55 (2013).
[12] A. F. Otte, M. Ternes, S. Loth, C. P. Lutz, C. F. Hirjibehedin, and A. J. Heinrich, Phys. Rev. Lett. **103**, 107203 (2009).
[13] A. Spinelli, M. Gerrits, R. Toskovic, B. Bryant, M. Ternes, and A. F. Otte, arXiv:1411.4415v2.
[14] B. Bryant, A. Spinelli, J. J. T. Wagenaar, M. Gerrits, and A. F. Otte, Phys. Rev. Lett. **111**, 127203 (2013).
[15] B. Bryant, R. Toskovic, A. Ferrón, J. L. Lado, Anna Spinelli, J. Fernández-Rossier, and A. F. Otte, Nano Lett. **15**, 6542 (2015).
[16] M. Persson, Phys. Rev. Lett. **103**, 050801 (2009).
[17] B. Sothmann and J. Konig, New J. Phys **12**, 083028 (2010).
[18] J. Fransson, O. Eriksson, and A. V. Balatsky, Phys. Rev. B **81**, 115454 (2010).
[19] A. Hurley, N. Baadji, and S. Sanvito, Phys. Rev. B **84**, 115435 (2011).
[20] N. Lorente and J. P. Gauyacq, Phys. Rev. Lett. **103**, 176601 (2009).
[21] J.-P. Gauyacq, N. Lorente, and F. D. Novaes, Prog. Surf. Sci. **87**, 63 (2012).
[22] M. Ternes, New J. Phys. **17**, 063016 (2015).
[23] M. Ternes, Prog. Surf. Sci. **92**, 1 (2017).
[24] P. Jacobson, T. Herden, M. Muenks, G. Laskin, O. Brovko, V. Stepanyuk, M. Ternes, and K. Kern, Nat. Commun. **6**, 8536 (2015).
[25] J. Fernández-Rossier, Phys. Rev. Lett. **102**, 256802 (2009).
[26] F. Delgado and J. Fernández-Rossier, Phys. Rev. B **82**, 134414 (2010).
[27] F. Delgado and J. Fernández-Rossier, Phys. Rev. B **84**, 045439 (2011).
[28] R. Zitko and Th. Pruschke, New J. Phys. **12**, 063040 (2010).
[29] J. Oberg, R. Calvo, F. Delgado, D. Jacob, M. Moro, D. Serrate, J. Fernández-Rossier, and C. Hirjibehedin, Nat. Nanotechnol. **9**, 64 (2014).
[30] D. Jacob and J. Fernández-Rossier, Eur. Phys. J. B **89**, 210 (2016).
[31] J. Kondo, Prog. Theor. Phys. **32**, 37 (1964).
[32] T. Pruschke and N. Grewe, Z. Phys. B **74**, 439 (1989).
[33] E. C. Goldberg and F. Flores, Phys. Rev. B **77**, 125121 (2008).
[34] E. C. Goldberg and F. Flores, J. Phys.: Condens. Matter **25**, 225001 (2013).
[35] E. C. Goldberg and F. Flores, Phys. Rev. B **91**, 165408 (2015).
[36] A. Yoshimori, Prog. Theor. Phys. **55**, 67 (1976).
[37] J. Hubbard, Proc. R. Soc. A **285**, 542 (1965).
[38] L. L. Hirst, Adv. Phys. **27**, 231 (1978).
[39] Y. V. Nazarov and Y. M. Blanter, *Quantum Transport: Introduction to Nanoscience* (Cambridge University Press, Cambridge, UK, 2009).
[40] J. Nicklas, A. Wadehra, and J. Wilkins, J. Appl. Phys. **110**, 123915 (2011).
[41] M. Etzkorn *et al.*, Phys. Rev. B **92**, 184406 (2015).
[42] J. R. Schrieffer and P. A. Wolf, Phys. Rev. **149**, 491 (1966).
[43] C. Jayaprakash, H. R. Krishna-murthy, and J. W. Wilkins, Phys. Rev. Lett. **47**, 737 (1981).
[44] J. Bardeen, Phys. Rev. Lett. **6**, 57 (1961).
[45] J. M. Blanco, F. Flores, and R. Perez, Prog. Surf. Sci. **81**, 403 (2006).
[46] F. Flores and E. C. Goldberg , in *Many-body Approaches at Different Scales*, edited by G. G. N. Angilella and C. Amovilli (Springer, New York) (unpublished).